Séminaire LMT – 21 février 2013

Lagrange-remap solver and low-diffusive interface capturing for air-water flows

Aude Bernard-Champmartin, Florian De Vuyst

Centre de Mathématiques et de leurs Applications
CMLA UMR 8536 – ENS CACHAN

Outline

1. Context, applications
2. System derivation
3. Numerical method
4. Antidiffusive procedure for the gas-liquid interface
5. Numerical experiments & validation
6. Concluding remarks

Context, applications

- Air-water flows, violent flow conditions
- Fast dynamics, transient regime

- Applications : Liquified Natural Gas LNG carriers, hydrodynamics, coastal engineering, wave impact, ...

Wave impact pressure peak analysis →

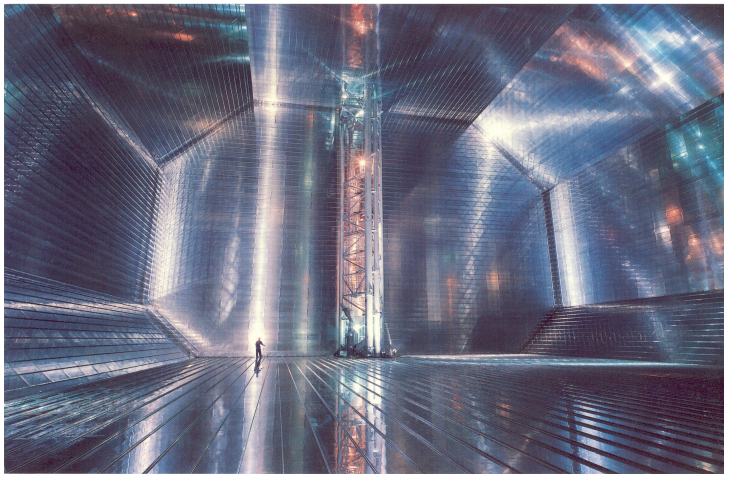

LNG carrier tank

Objectives

- Design numerical methods subject to some requirements :
  - Robustness
  - Accuracy
  - Conservation
  - Fluid treated as compressible
  - **Natural parallel extension / implementation**

- Accelerate computations to 2 or 3 orders of magnitude, allowing for statistics (as for experimental setups, hexapods)

Sources of stiffness

- Gas/liquid mass density ratio of order 1000
- Stiffness due to weak compressibility of liquid → low Mach number flows
- Gas-liquid free boundaries

Assumptions here

- Viscous effects omitted
- Surface tension omitted

Derivation of the system (inviscid)

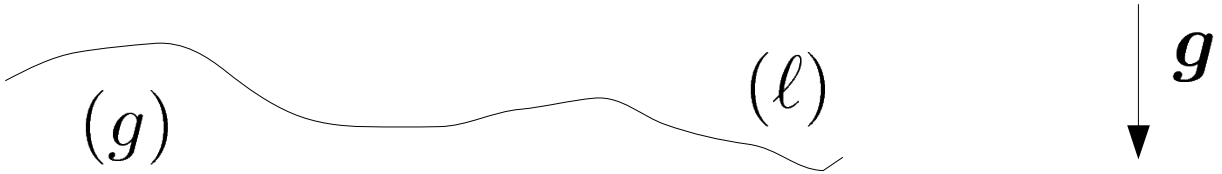

$$\partial_t \rho_k + \nabla \cdot (\rho_k \boldsymbol{u}) = 0$$
$$\partial_t (\rho_k \boldsymbol{u}) + \nabla \cdot (\rho_k \boldsymbol{u} \otimes \boldsymbol{u}) + \nabla p = \rho_k \boldsymbol{g}, \quad k = g, \ell$$

Indicator function : $z = z(\boldsymbol{x}, t) \in \{0, 1\}$ $\rho = z\rho_g + (1 - z)\rho_\ell$

$$\partial_t \rho + \nabla \cdot (\rho \boldsymbol{u}) = 0,$$
$$\partial_t (\rho \boldsymbol{u}) + \nabla \cdot (\rho \boldsymbol{u} \otimes \boldsymbol{u}) + \nabla p = \rho \boldsymbol{g},$$
$$D_t z = \partial_t z + \boldsymbol{u} \cdot \nabla z = 0,$$
$$p = z\, p_\ell(\rho_\ell) + (1 - z)\, p_g(\rho_g) \qquad \frac{\partial p_k}{\partial \rho_k} = c_k^2 > 0$$

Involving gas mass fraction

$$c_g \in \{0, 1\}$$

$$\partial_t(c_g\rho) + \nabla \cdot (c_g\rho\boldsymbol{u}) = 0$$

From

$$\partial_t\rho + \nabla \cdot (\rho\boldsymbol{u}) = 0,$$

we also get

$$D_t c_g = \partial_t c_g + \boldsymbol{u} \cdot \nabla c_g = 0.$$

Dealing with numerical *z* in *[0,1]*

$$\partial_t \rho + \nabla \cdot (\rho \boldsymbol{u}) = 0,$$ Total mass conservation

$$\partial_t (\rho \boldsymbol{u}) + \nabla \cdot (\rho \boldsymbol{u} \otimes \boldsymbol{u}) + \nabla p = \rho \boldsymbol{g},$$ Momentum balance

$$\partial_t (c_g \rho) + \nabla \cdot (c_g \rho \boldsymbol{u}) = 0,$$ Gas mass conservation

$$D_t z = \partial_t z + \boldsymbol{u} \cdot \nabla z = 0,$$

$$p = z\, p_\ell(\rho_\ell) + (1 - z)\, p_g(\rho_g)$$ Pressure closure

In the spirit of [Kokh-Lagoutière 2010]

Introducing the volume fraction :

$$z\rho_g = c_g \rho, \quad z\rho_g + (1 - z)\rho_\ell = \rho.$$

Shorcoming: $\rho_g = \dfrac{c_g \rho}{z}$ may be undetermined numerically.

Use of a (simplified) volume-averaged system and pressure equilibrium closure

$$\partial_t \rho + \nabla \cdot (\rho \boldsymbol{u}) = 0,$$

$$\partial_t (\rho \boldsymbol{u}) + \nabla \cdot (\rho \boldsymbol{u} \otimes \boldsymbol{u}) + \nabla p = \rho \boldsymbol{g},$$

$$\partial_t (c_g \rho) + \nabla \cdot (c_g \rho \boldsymbol{u}) = 0,$$

$$p = p_g(\rho_g) = p_\ell(\rho_\ell)$$ Pressure equilibrium into an elementery volume

can be rewritten as

$$\partial_t \big(\alpha \rho_g\big) + \nabla \cdot (\alpha \rho_g \boldsymbol{u}) = 0,$$

$$\partial_t \big((1-\alpha) \rho_\ell\big) + \nabla \cdot \big((1-\alpha) \rho_\ell \boldsymbol{u}\big) = 0,$$

$$\partial_t (\rho \boldsymbol{u}) + \nabla \cdot (\rho \boldsymbol{u} \otimes \boldsymbol{u}) + \nabla p = \rho \boldsymbol{g},$$

$$p = p_g(\rho_g) = p_\ell(\rho_\ell)$$

Typical equations of state (EOS) in use

$$p_g(\rho_g) = p_0 \left(\frac{\rho_g}{\rho_g^0}\right)^{\gamma_g}, \ \gamma_g = 1.4,$$

$$p_\ell(\rho_\ell) = p_0 + \frac{\rho_\ell^0 c_s^2}{\gamma_\ell}\left(\left(\frac{\rho_\ell}{\rho_\ell^0}\right)^{\gamma_\ell} - 1\right), \ \gamma_\ell = 7.$$

Near atmospheric conditions :

$$p_0 = 10^5 \ Pa, \ \rho_g^0 = 1.2 \ kg.m^{-3}, \ \rho_l^0 = 1000 \ kg.m^{-3}.$$

$$c_s = 1500 \ m.s^{-1}. \ \text{Artificial: } c_s = 350 \ m.s^{-1}.$$

Pressure equilibrium equation

- From the knowledge of the conservative variables $W_g = \alpha\rho_g$ and $W_g = (1-\alpha)\rho_g$, we have to solve :

$$p_g(\rho_g) = p_\ell(\rho_\ell)$$

i.e.

$$\varphi(\alpha) = \left(\frac{W_g}{\alpha\rho_g^0}\right)^{\gamma_g} - 1 - K\left[\left(\frac{W_\ell}{(1-\alpha)\rho_\ell^0}\right)^{\gamma_\ell} - 1\right] = 0, \quad \alpha \in]0,1[.$$

- NB : very stiff function, the choice of the iterative solver requires attention (initial guess, surrogates, Newton, etc.)

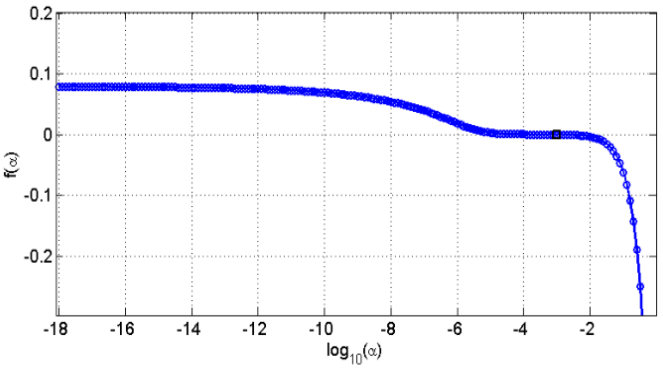

In fact, there is a trick … :

Trick for initial guess :

- The liquid mass conservation equation can be written in conservative form as :

$$\partial_t(1-\alpha) + \nabla \cdot [(1-\alpha)\boldsymbol{u}] = -\frac{D_t \rho_\ell}{\rho_\ell}.$$

- Under the *weak compressibility assumption* or the liquid phase, we get

$$\partial_t \alpha + \nabla \cdot (\alpha \boldsymbol{u}) = 0.$$

- A numerical scheme is applied to this additional ``guess equation'' to compute initial guesses of the iterative solver

  $\rightarrow$ Newton algorithm converges in 2 iterates with acceptable accuracy (strong improvement in CPU time).

Numerical scheme

Remapped Lagrange Eulerian solver

- First write the equations in Lagrange form

$$\rho\, D_t\Big(\frac{1}{\rho}\Big) - \nabla\cdot\boldsymbol{u} = 0,$$

$$\rho\, D_t\boldsymbol{u} + \nabla p = \boldsymbol{g},$$

$$D_t c_g = 0,$$

$$\frac{d}{dt}\int_{\Omega_t} \alpha\rho_g\, dx = 0,$$

$$\frac{d}{dt}\int_{\Omega_t} (1-\alpha)\rho_\ell\, dx = 0,$$

$$\frac{d}{dt}\int_{\Omega_t} \rho\boldsymbol{u}\, dx + \int_{\Omega_t} \nabla p\, dx = \int_{\Omega_t} \rho\boldsymbol{g}.$$

- Advance in time
- Project the quantities on the fixed Eulerian grid (remap)

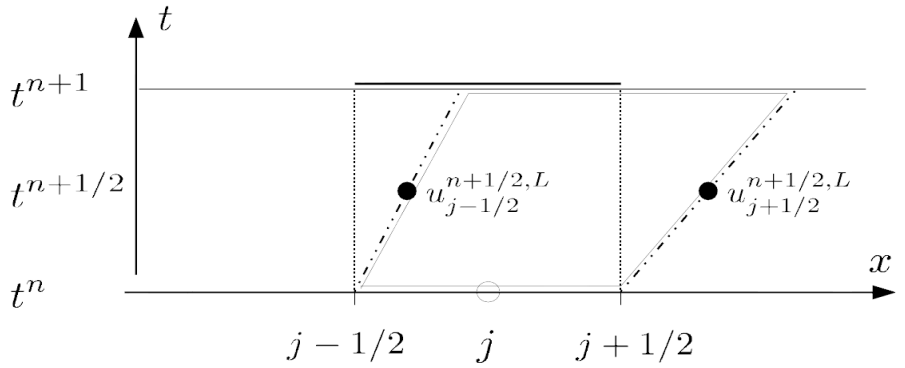

Typical Lagrange scheme (spatial staggered grid)

$$u_{i+1/2,j}^{n+1/2,L} = u_{i+1/2,j}^{n} - \frac{\Delta t}{2}\frac{\Delta y}{m_{i+1/2,j}^{n}}\left[(p+q)_{i+1,j}^{n+1/2,L} - (p+q)_{i,j}^{n+1/2,L}\right],$$

$$v_{i,j+1/2}^{n+1/2,L} = v_{i,j+1/2}^{n} - \frac{\Delta t}{2}\frac{\Delta x}{m_{i,j+1/2}^{n}}\left[(p+q)_{i,j+1}^{n+1/2,L} - (p+q)_{i,j}^{n+1/2,L}\right] + \frac{\Delta t}{2}g.$$

$$V_{i,j}^{n+1,L} = V_{i,j}^{n} + \Delta t\Delta y\left(u_{i+1/2,j}^{n+1/2,L} - u_{i-1/2,j}^{n+1/2,L}\right) + \Delta t\Delta x\left(v_{i,j+1/2}^{n+1/2,L} - v_{i,j-1/2}^{n+1/2,L}\right).$$

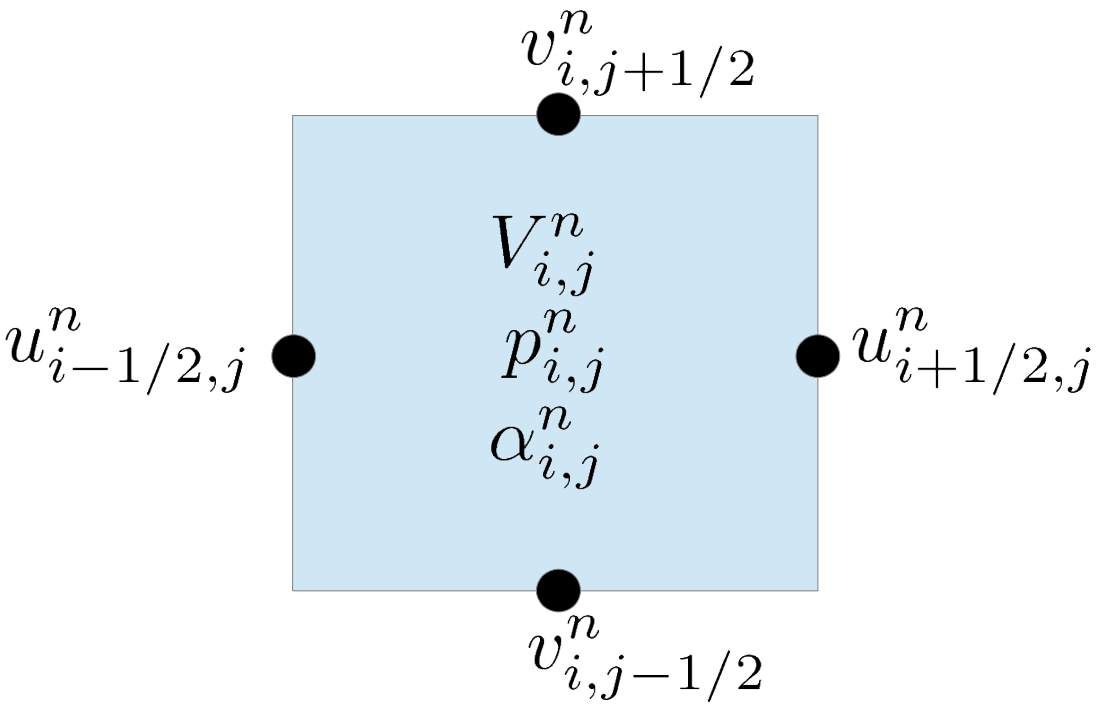

A short walk on Lagrange-remap (Euler 1D)

Lagrange step :

$$\rho_j^{n+1,L} V_j^{n+1,L} = \rho_j^n V_j^n$$

Pseudo-viscosity

$$V_j^{n+1,L} = V_j^n + \Delta t(u_{j+1/2}^{n+1/2,L} - u_{j-1/2}^{n+1/2,L})$$

$$m_{j+1/2}^n u_{j+1/2}^{n+1,L} = m_{j+1/2}^n u_{j+1/2}^n - \Delta t(\Delta p_{j+1/2}^{n+1/2,L} + \Delta q_{j+1/2}^{n+1/2,L})$$

"$de + pd\tau$"

$$e_j^{n+1,L} = e_j^n - \frac{p_j^{n+1/2,L} + q_j^{n+1/2,L}}{m_j^n}(V_j^{n+1,L} - V_j^n)$$

$$\frac{e_j^{n+1,L} - e_j^n}{\Delta t} + \frac{p_j^{n+1/2,L}}{m_j^n}(u_{j+1/2}^{n+1/2,L} - u_{j-1/2,L}^{n+1/2,L}) = -\frac{q_j^{n+1/2,L}}{m_j^n}(u_{j+1/2}^{n+1/2,L} - u_{j-1/2,L}^{n+1/2,L})$$

$$\begin{aligned} q_j^{n+1/2,L} &\propto -(u_{j+1/2}^{n+1/2,L} - u_{j-1/2}^{n+1/2,L}) \\ &= -\beta(\rho c^2)_j^{n+1/2,L} \Delta u_j^{n+1/2,L} \end{aligned}$$

A short walk on Lagrange-remap ...

- Lagrange step : entropy-satisfying

- Projection step : dissipative process due to Jensen's inequality (consider convex entropies) …

=> rather simple process with positivity & entropy properties, does not require any approximate Riemann solver.

Conservative form

- Lagrange-remap schemes actually can be rewritten in conservative form [De Vuyst et al, preprint 2013].
- 1D case :

$$(\alpha\rho_g)_j^{n+1} = (\alpha\rho_g)_j^{n+1} - \frac{\Delta t}{h}\left[(\Phi_{m,g})_{j+1/2}^{n,n+1} - (\Phi_{m,g})_{j-1/2}^{n,n+1}\right],$$

$$(\Phi_{m,g})_{j+1/2}^{n,n+1} = \alpha_{j+1/2}^{n+1,L}\,(\rho_g)_{j+1/2}^{n+1,L}\,u_{j+1/2}^{n+1/2,L}$$

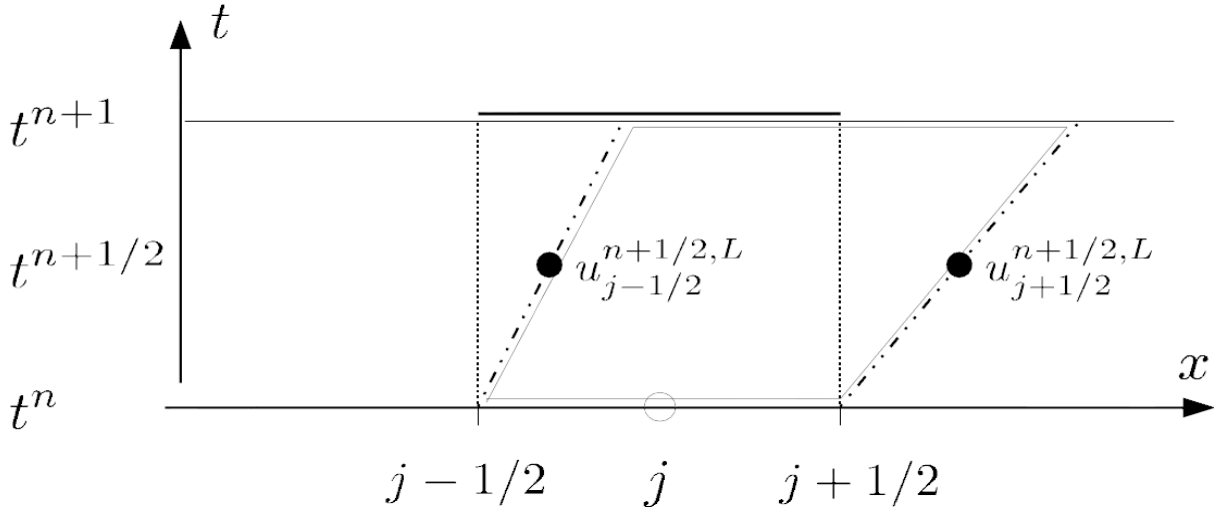

Antidiffusive strategy

$$(\alpha\rho_g)_j^{n+1} = (\alpha\rho_g)_j^{n+1} - \frac{\Delta t}{h}\left[(\Phi_{m,g})_{j+1/2}^{n,n+1} - (\Phi_{m,g})_{j-1/2}^{n,n+1}\right],$$

$$(\Phi_{m,g})_{j+1/2}^{n,n+1} = \alpha_{j+1/2}^{n+1,L}\,(\rho_g)_{j+1/2}^{n+1,L}\,u_{j+1/2}^{n+1/2,L}$$

Void fraction at interface : how to compute it ?

- Strategy : « be as most accurate as possible for step-shaped color functions while being stable (just at the limit) »
- Idea : design a combination of upwind scheme and downwind scheme [Lagoutière Després 2002, Kokh-Lagoutière 2010]
- The advection process can be seen as a over-compressive « limiting » procedure (superbee-like, hyperbee, ...)

Upwinding (stable but diffusive) vs downwinding (anti-diffusive but unstable) ...

Transport of the mass gas fraction : $\partial_t c_g + \boldsymbol{u} \cdot \nabla c_g = 0$

- Consistency requirement

$$(c_g)_{i+1/2,j} \in [min((c_g)_{i,j}, (c_g)_{i+1,j}),\ max((c_g)_{i,j}, (c_g)_{i+1,j})]$$

- Stability requirement

  « do not produce new extrema, discrete local maximum principle »

- Take the value closest to the downwind one while being in the trust interval.

Some theoretical results

Theorem 4.1. *Under the condition to be respected by the time step (in which* $s = sign(u_{i+1/2}^{n+1/2,L})$*)*

$$V_{i+1/2,j,upw}^{n+1,*} - s\Delta t\Delta y\, u_{i+1/2-s,j} \geq 0, \tag{59}$$

when $u_{i+1/2,j}^{n+1,L} u_{i+s/2,j}^{n+1,L} > 0$ *(i.e. when the velocities at the edges of the cell where the stability condition is calculated are of the same sign), the value of* $\alpha_{i+1/2,j}^{LowDiff}$ *can be taken in the following* trust interval I*:*

$$I = \underbrace{I_1}_{\text{flux consistency for } c_g} \cap \underbrace{I_2^s}_{\text{stability for } c_g} := [\omega_{i+1/2,j}^{n+1,L}, \Omega_{i+1/2,j}^{n+1,L}] \in [0,1], \tag{60}$$

which is not empty since the upwind value $\alpha_{i+1/2,j,up}^{n+1,L} \in I$*, where the interval* I_1 *are defined by (44) and* I_2^s *by (48)-(49) (or written in a generic form (C.1)-(C.2)). Moreover, taking* $\alpha_{i+1/2,j}^{LowDiff} \in I$ *ensures to respect maximum principle on* c_g *and especially to keep the positivity of the masses of each phases during the projection.*

Test cases

and numerical experiments

(+ comparison to physical experiments
for some of them)

1. Collapse of a liquid column with an obstacle

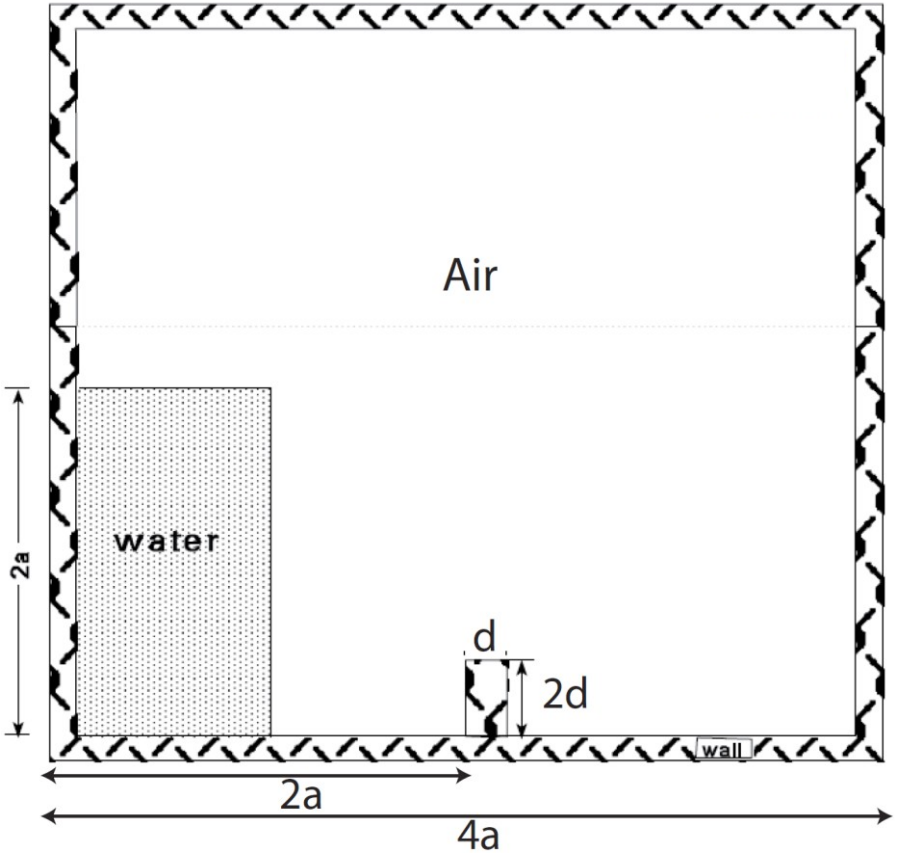

O. Ubbink Numerical prediction of two-fluid systems with sharp interfaces, PhD thesis (1997)

$$a = 0.146 \text{ m},\ d = 0.024 \text{ m}$$

$$Nx = Ny = 150$$

$$\gamma_g = 1.4,\ \gamma_l = 7$$

$$\rho_0^g = 1.28 \text{ kg.m}^{-3},\ \rho_0^l = 1000 \text{ kg.m}^{-3}$$

$$P_0 = 10^5,\ c_{\text{sound}} = 350 \text{ m.s}^{-1}$$

Collapse with an obstacle – comparison with incompressible fluid model

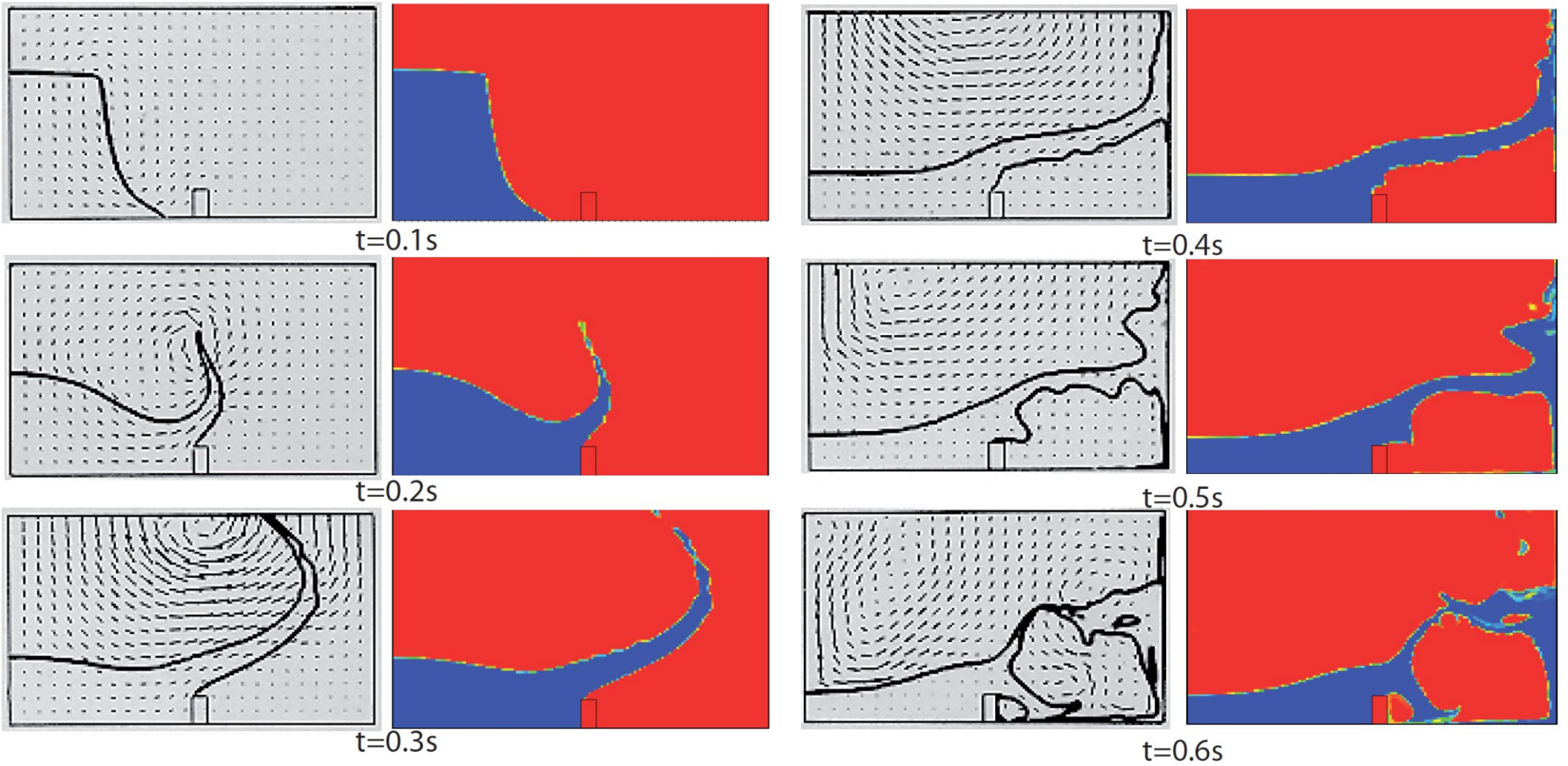

Num. Result. Ubbink

Num. Result. with Odyssey

Num. Result. Ubbink

Num. Result. with Odyssey

Benefits of the antidiffusive approach

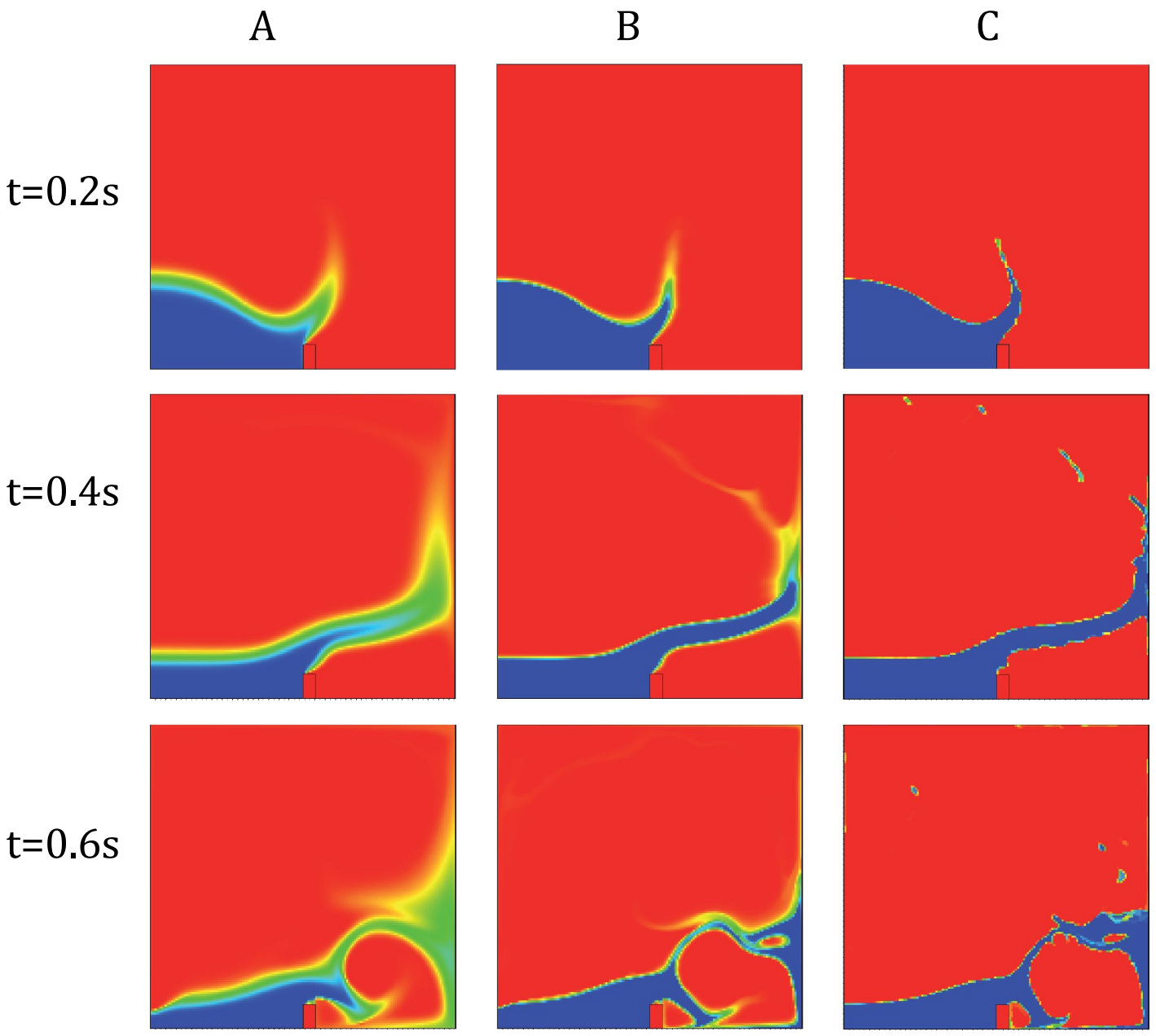

Evolution of □ for different remapping algorithms

- ✓Case A: 1st order with upwind
- ✓Case B: 2nd order with upwind
- ✓Case C: 1st order with Low-Diff.

Gas mass fraction : numerical diffusion appears due to filamentation / fragmentation

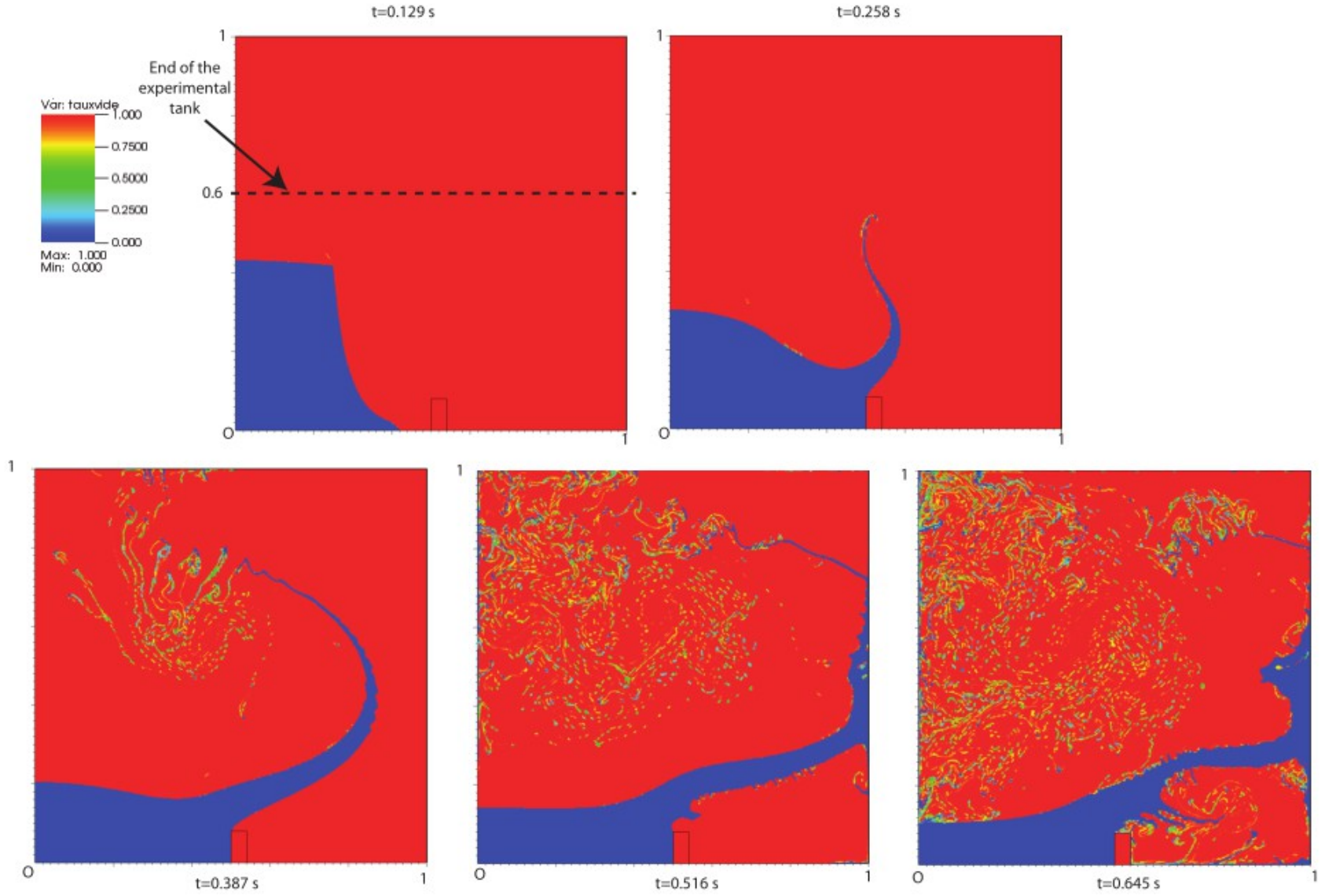

Velocity vector field

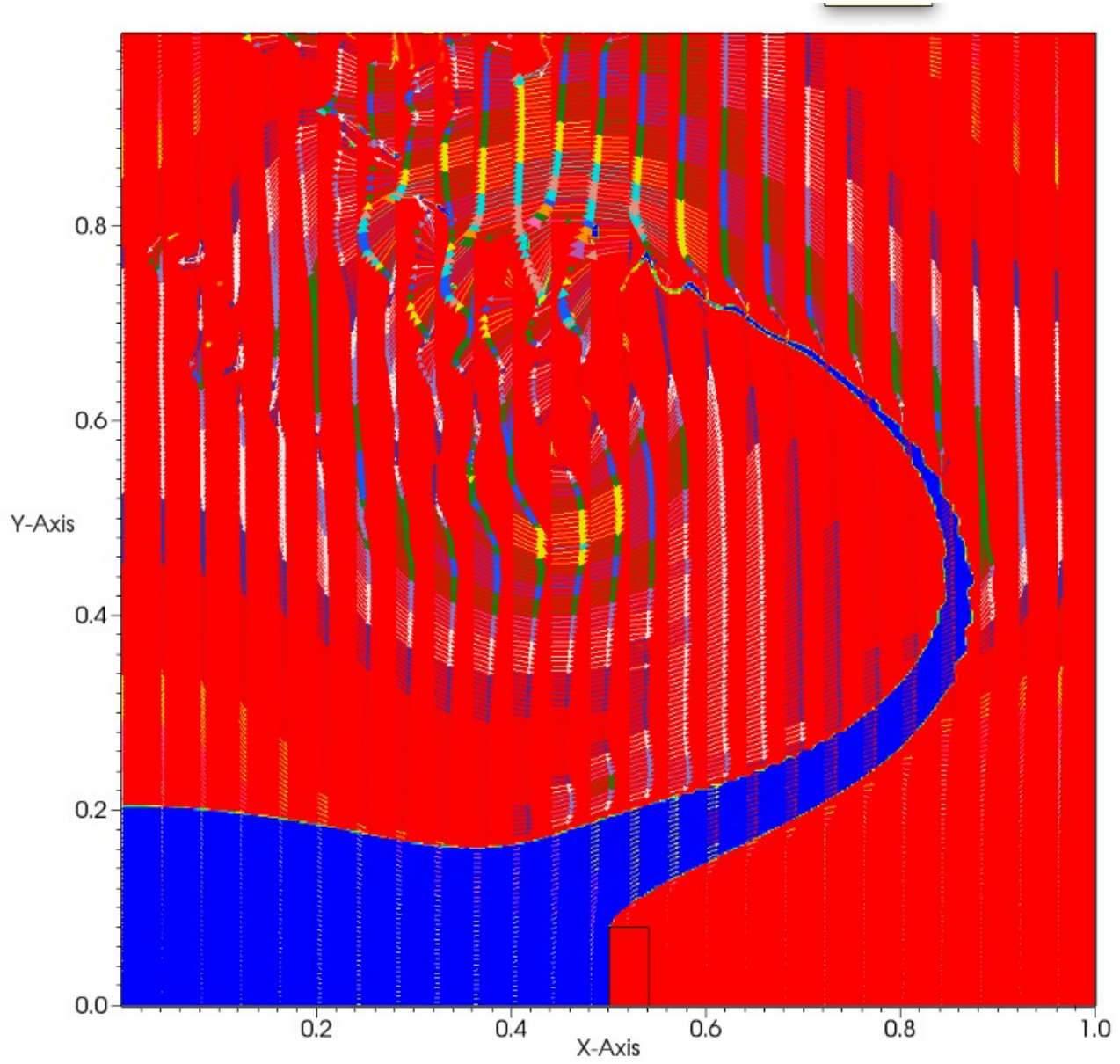

- Another case of collapse of a liquid column with an obstacle

D. M. Greeves Simulation of viscous water column collapse using adapting hierarchical grids J. Num. Meth. Fluids 2006

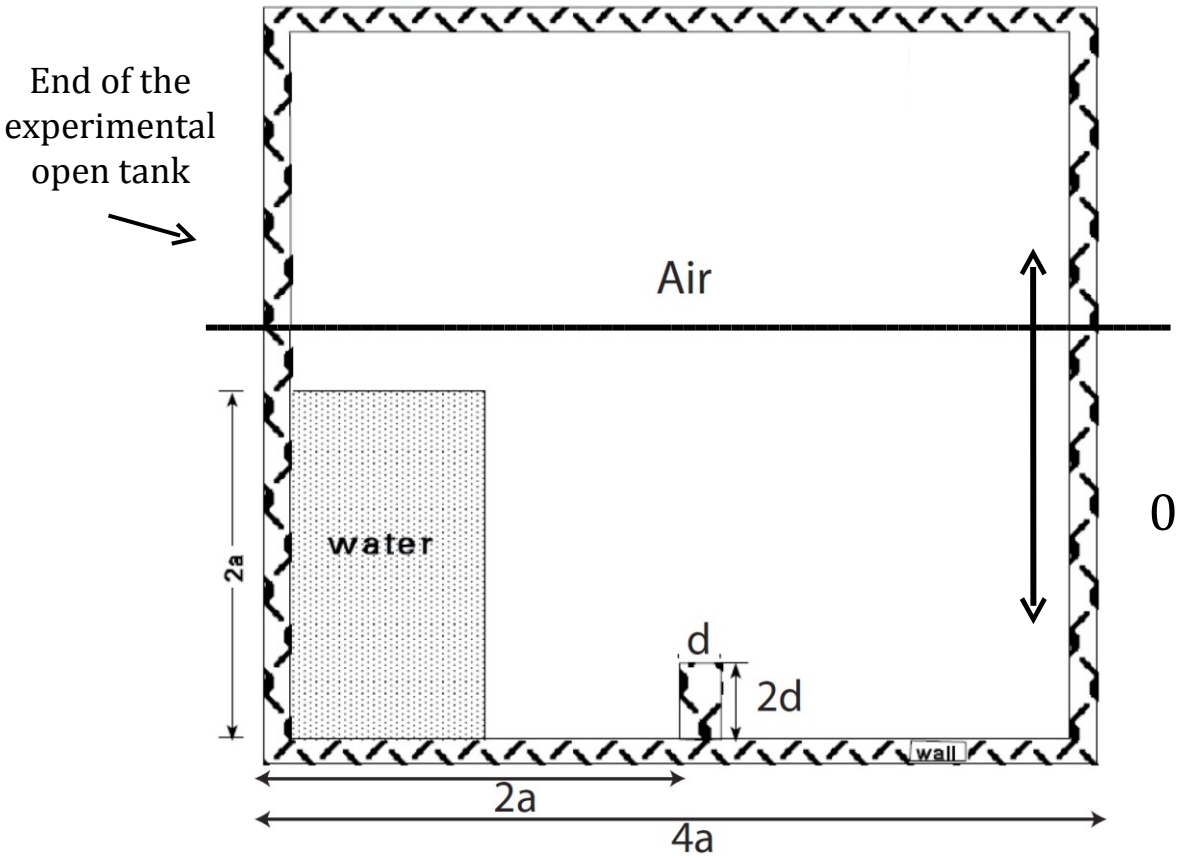

$$a = 0.25,\ d = 0.04$$

$$Lx = Ly = 1\ \text{m}$$

$$Nx = Ny = 300$$

$$\gamma_g = 1.4,\ \gamma_l = 7$$

$$\rho_0^g = 1.\ \text{kg.m}^{-3},\ \rho_0^l = 1000\ \text{kg.m}^{-3}$$

$$P_0 = 10^5,\ c_{\text{sound}} = 350\ \text{m.s}^{-1}$$

Exp: from

Koshizuka et al A particle method.. Comp. Fluid Mech. 1995

Simulations of a dam break

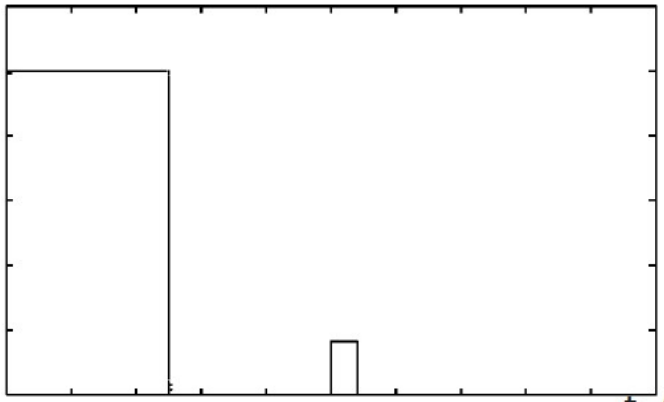

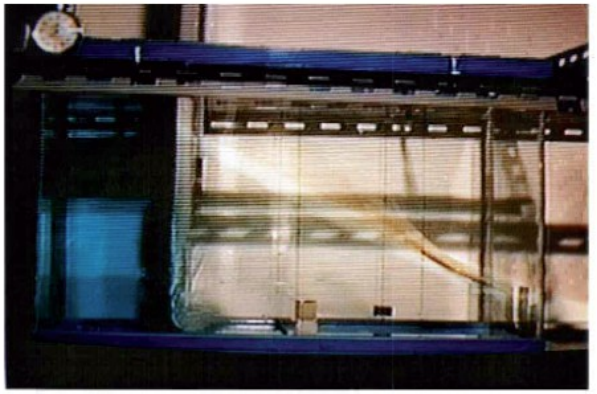

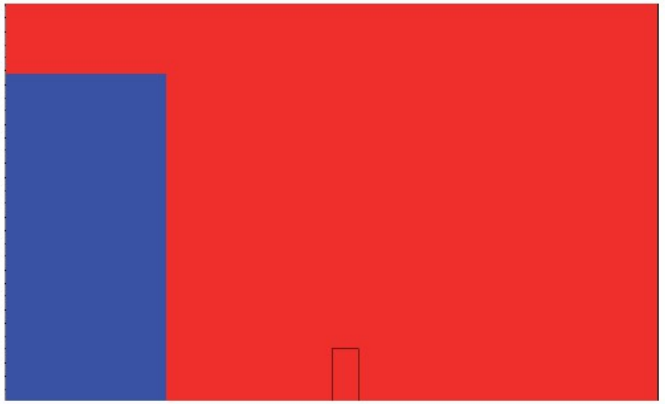

t=0s

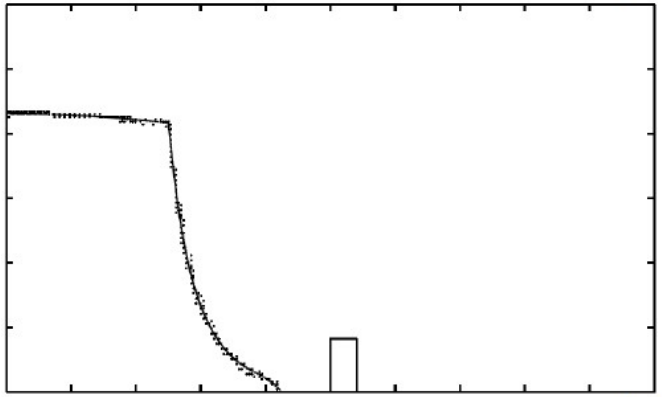

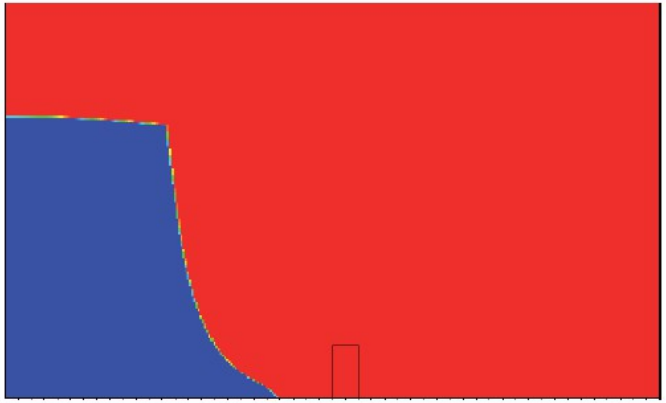

t=0.129s

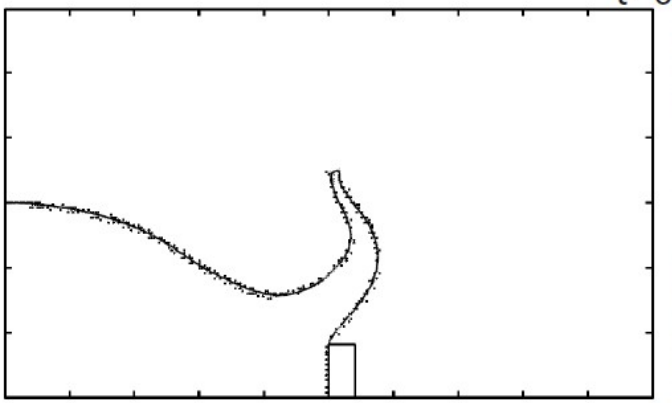

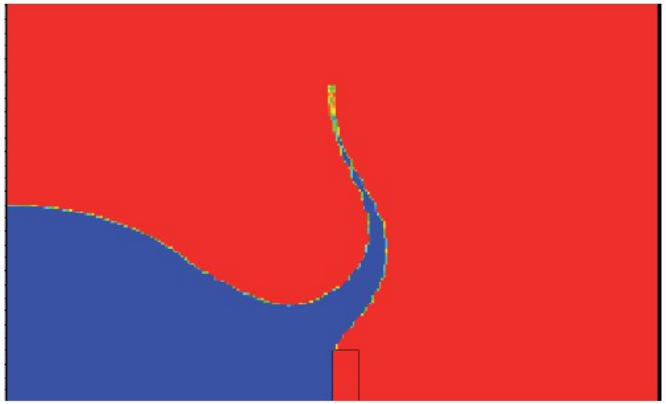

t=0.258s

Sim. Greeves

Exp. Koshizuka

Sim. Odyssey

Simulations of a dam break

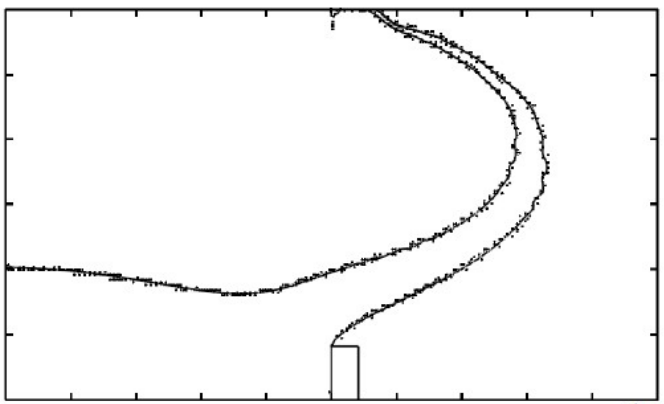

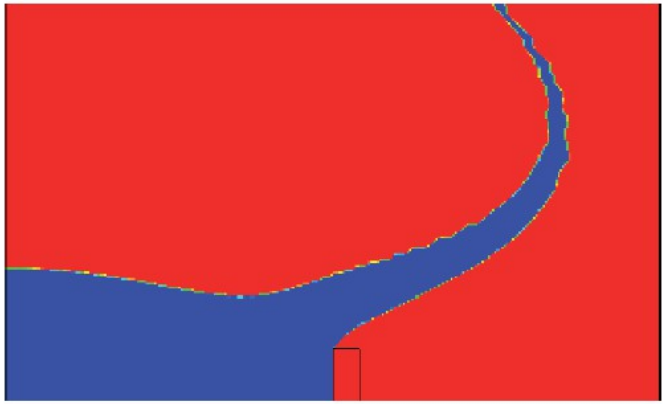

t=0.387s

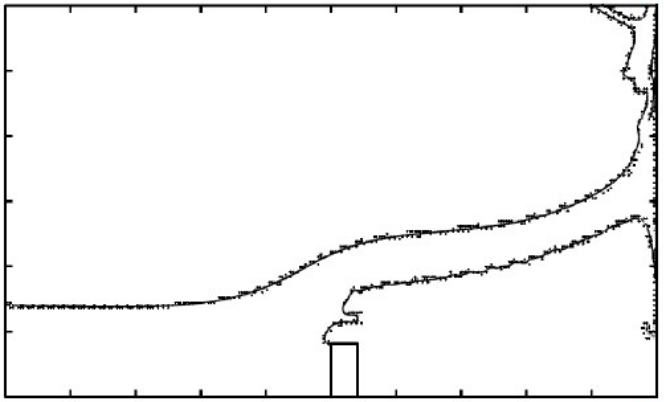

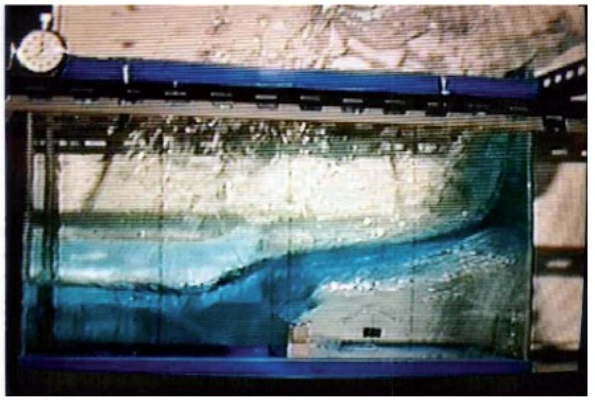

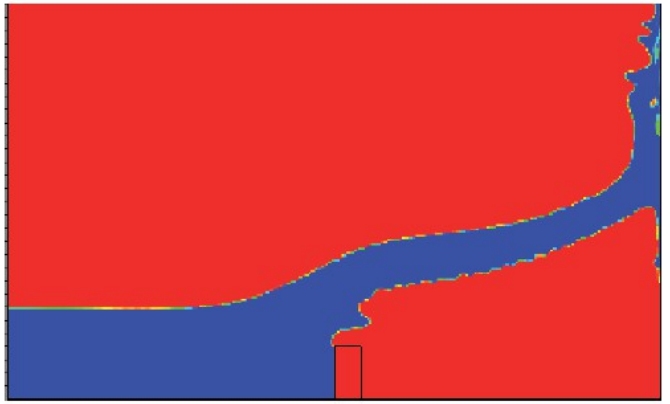

t=0.516s

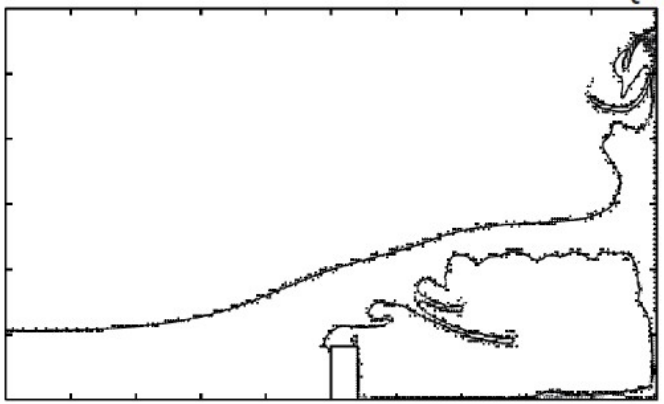

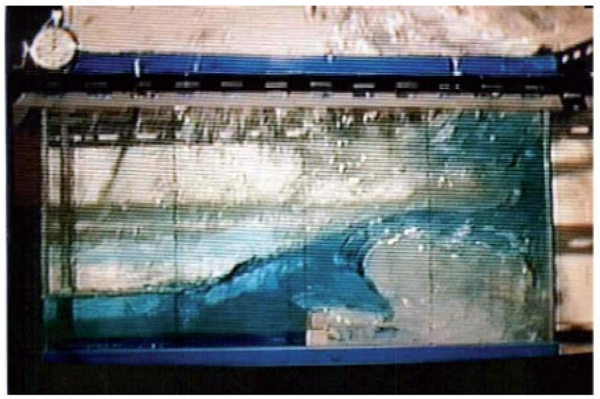

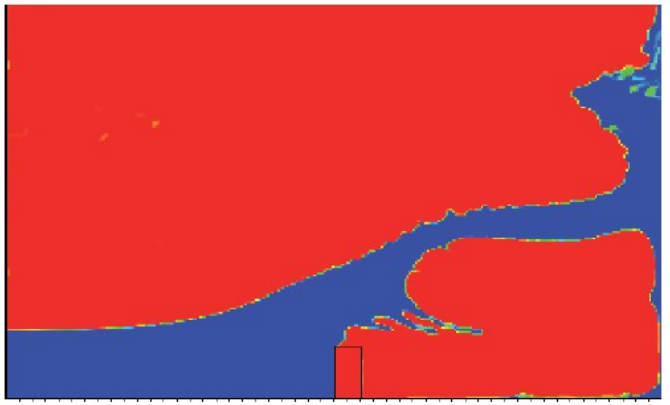

t=0.645s

Sim. Greeves

Exp. Koshizuka

Sim. Odyssey

Sloshing test cases – pitch motion

- Sloshing due to the **pitch motion** of a rectangular tank:

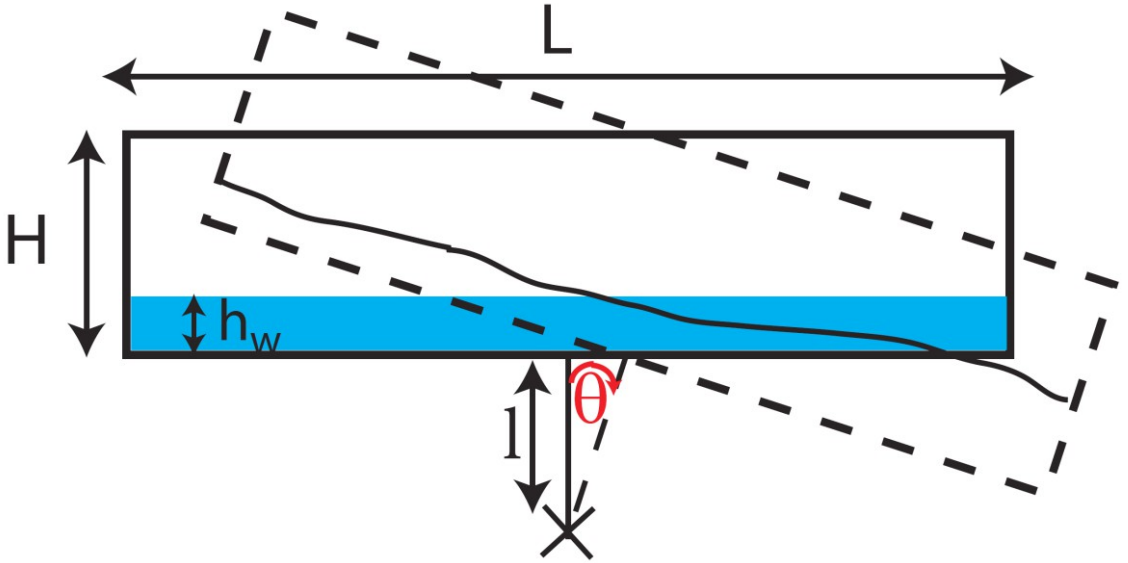

J.R. Shao *et al* . An improved SPH method for modeling liquid sloshing dynamics. Comp. Fluids 2012

$$L = 0.64m,\ H = 0.14m,\ h_w = 0.03m$$

$$Nx = 300,\ Ny = 67$$

The tank is oscillating as a **pendulum** according to:

$$\theta(t) = \theta_0 \sin(\omega_r t)$$

with $\theta_0 = 6^\circ,\ \omega_r = 4.34$ rad/s $(T = 1.45$ s$)$

Simulation are performed in the frame of reference of the tank.

Sloshing test cases – pitch motion

We superimpose the profile of the article:

J.R. Shao *et al* . An improved SPH method for modeling liquid sloshing dynamics. Comp. Fluids 2012

t_1=1.45s

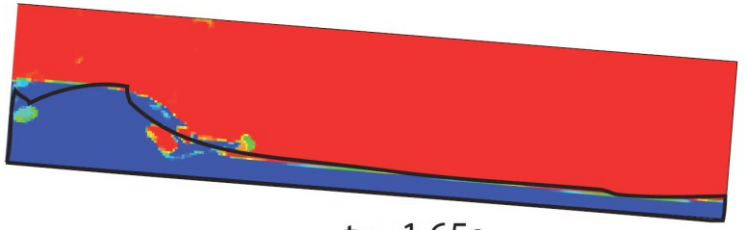

t_2=1.65s

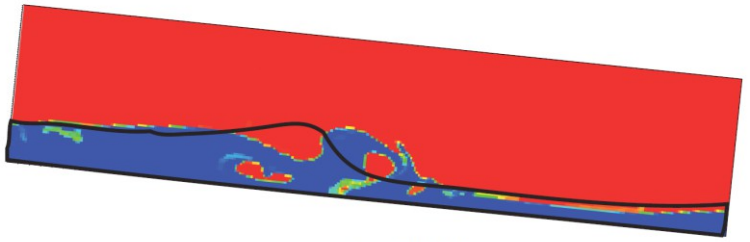

t_3=1.85s

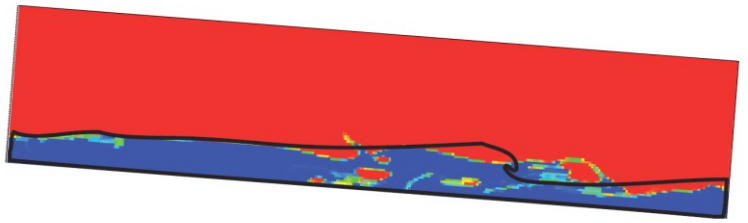

t_4=1.98s

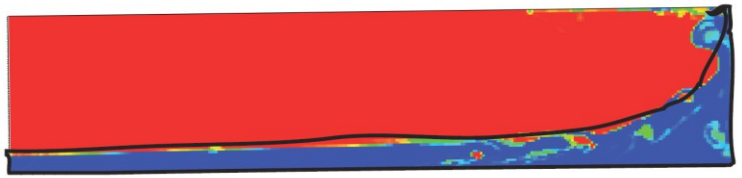

t_5=2.2s

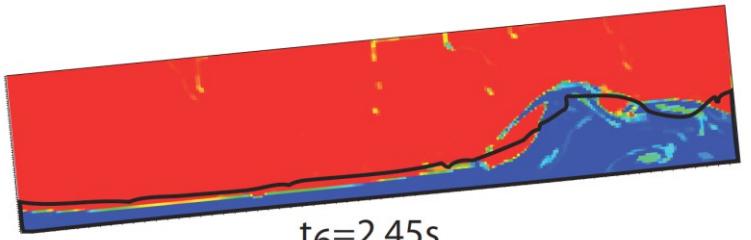

t_6=2.45s

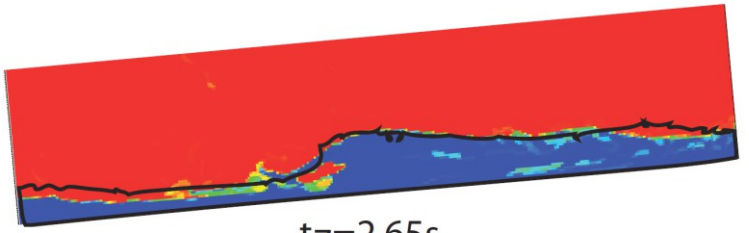

t_7=2.65s

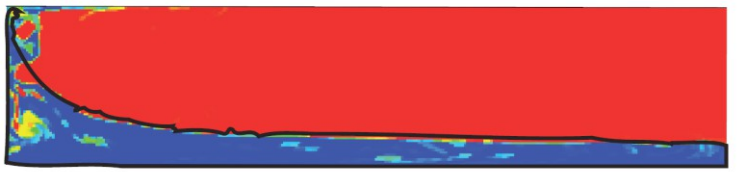

t_8=2.90s

Sloshing due to the **surge motion** of a rectangular tank:

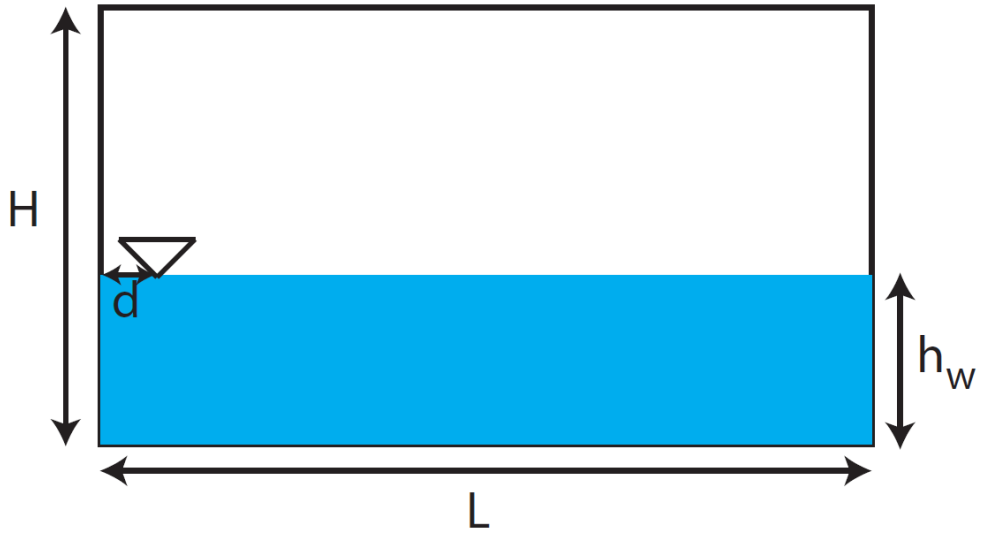

J.R. Shao *et al* . An improved SPH method for modeling liquid sloshing dynamics. Comp. Fluids 2012

$L = 1.73m,\ H = 1.15m,\ h_w = 0.6m$

$d = 0.05$ m

$Nx = 173,\ Ny = 115$

The tank is moving horizontally according to:

$$x(t) = A\cos\left(\frac{2\pi t}{T}\right)$$

with $A = 0.032$ m, $T = 1.3$ s (ω_{forced}=4.83 rad/s).

First natural frequency of the fluid in the box

$$\omega_{fluid} = \sqrt{g\frac{\pi}{L}\tanh(\frac{\pi}{L}h_w)} \approx 3.77 \text{ rad/s}$$

Two frequencies are acting ω_{fluid} and ω_{forced}

Experimental results available: **O.M. Faltinsen *et al* . Multidimensional modal analysis... J. Fluid. Mechanics 2000**

Sloshing test cases – surge motion

Free surface elevation of water at the probe

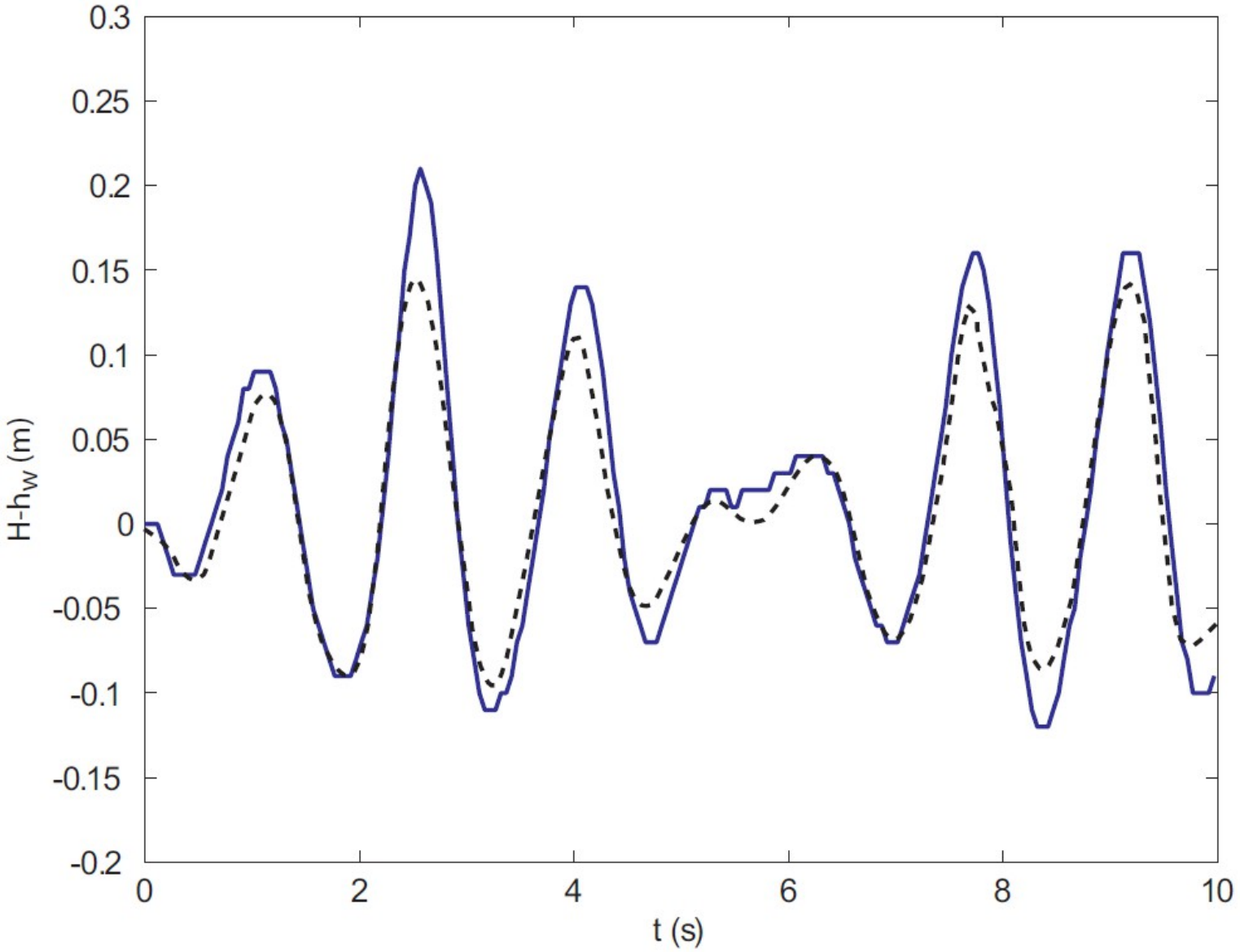

with our code

Scanned experimental results of

O.M. Faltinsen *et al* . Multidimensional modal analysis... J. Fluid. Mechanics 2000

Sloshing test cases – Surge motion

We search to **find a fit of** our curve with a function as a superposition of two signals

$$f(t) = A_1 \sin(f_1 t + \varphi_1) + A_2 \sin(f_2 t + \varphi_2)$$

we get: $f_1 = 3.74 \pm 0.01$ rad/s, $f_2 = 4.83 \pm 0.01$ rad/s

very close to $\omega_{fluid} \approx 3.77$ rad/s and $\omega_{forced} = 4.83$ rad/s

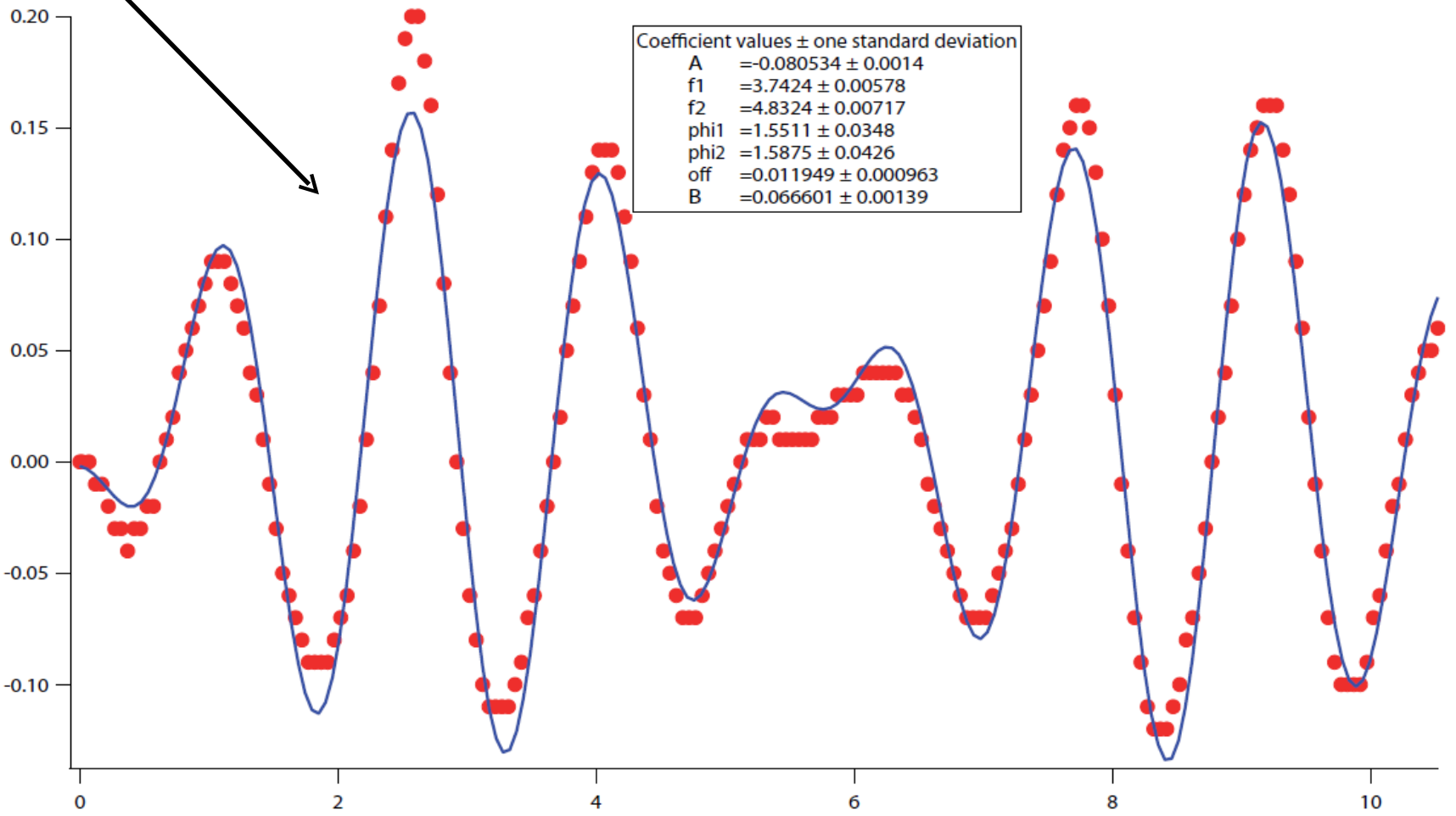

Free fall of liquid
and impact with liquid at rest

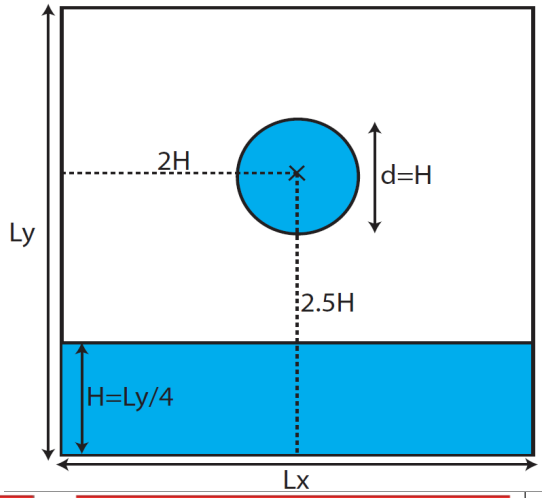

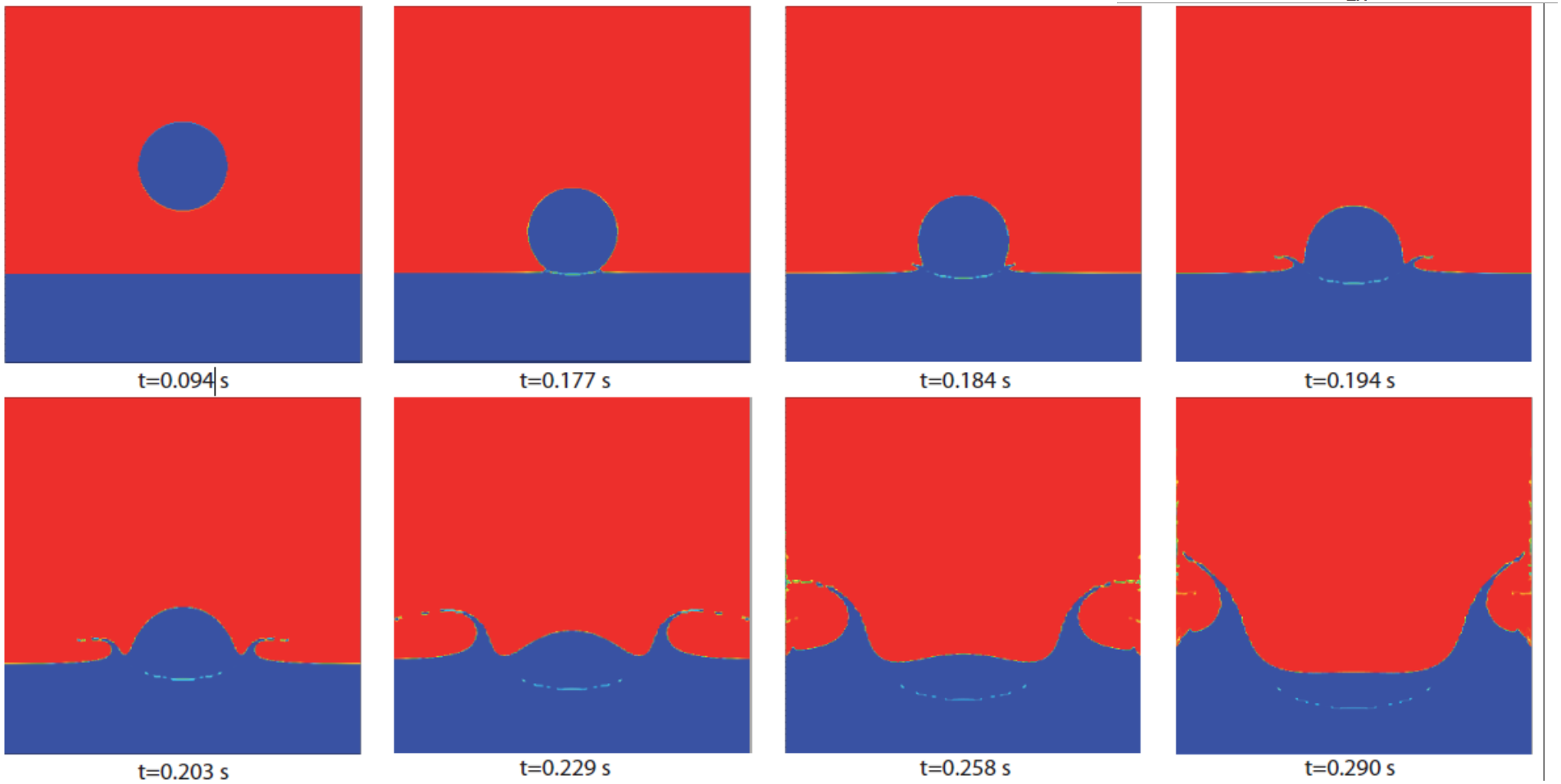

Liquid-liquid impact

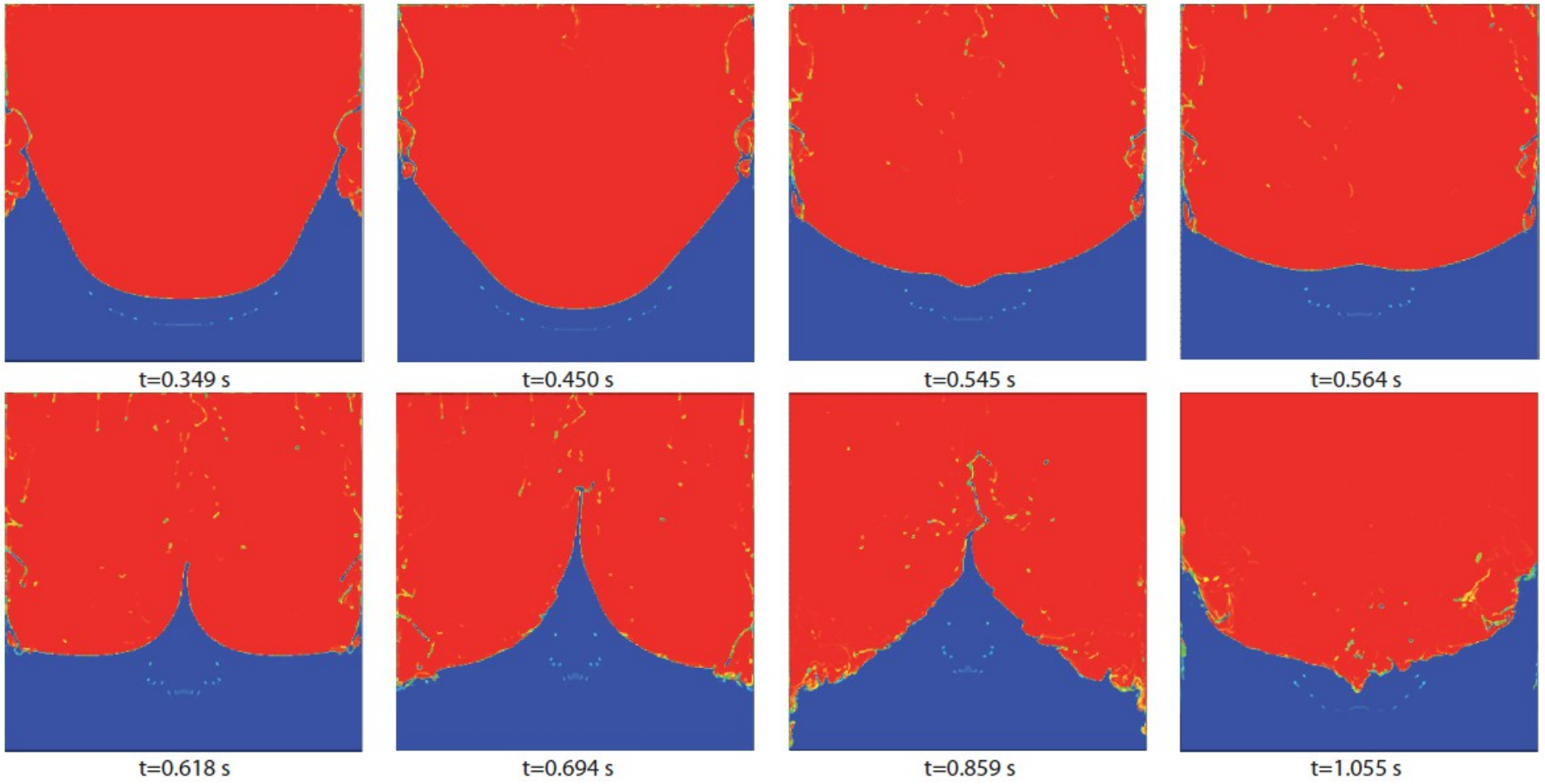

LT air-water Rayleigh-Taylor instability

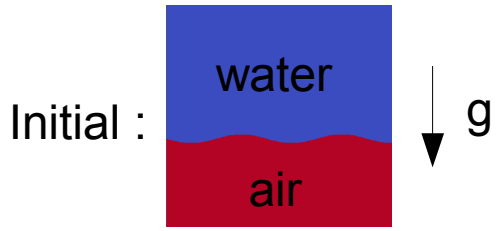

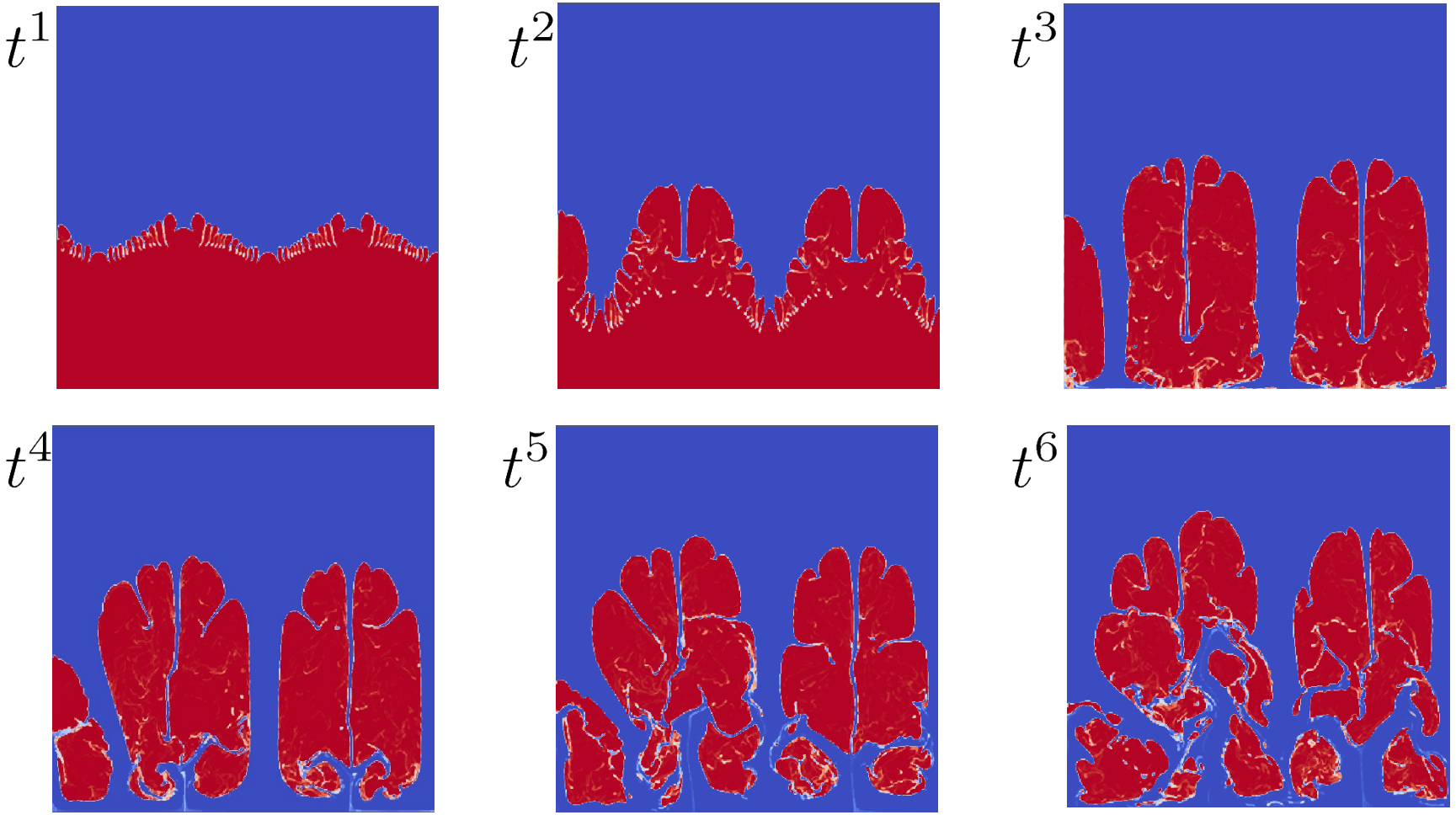

About 0.5 sec of physical time

Grid 400x400, about 1.5 day of computation (sequential)

Concluding remarks

- Innovative numerical Eulerian method involving :
  - a Lagrange-Remap finite volume method
  - an anti-diffusive approach on the gas mass/volume fraction
- The test cases show a good agreement between XP and other codes (dam break, sloshing events)

- Ongoing works : XP + num of water wave wall impact (L. Lenain, K. Melville, U. Delaware, Frédéric Dias, U. College Dublin).
- Need to add : physical viscosity, surface tension
- Graphics Processing Unit (GPU) implementation

Thank you for your attention

ENS CACHAN

Cmla

Lagrange-remap : conservative reformulation

i.e.

$$\rho_j^{n+1,L} = \frac{\rho_j^n}{1 + \frac{\Delta t}{h}(\Delta u)_j^{n+1/2,L}}, \quad (\Delta u)_j^{n+1/2,L} := u_{j+1/2}^{n+1/2,L} - u_{j-1/2}^{n+1/2,L}.$$

Projection step:

$$\rho_j^{n+1} = \frac{1}{h}\int_{I_j} \mathscr{I}\rho^{n+1,L}(x)\,dx = \frac{1}{h}\int_{I_j^{n+1,L}} \ldots - \ldots + \ldots \,.$$

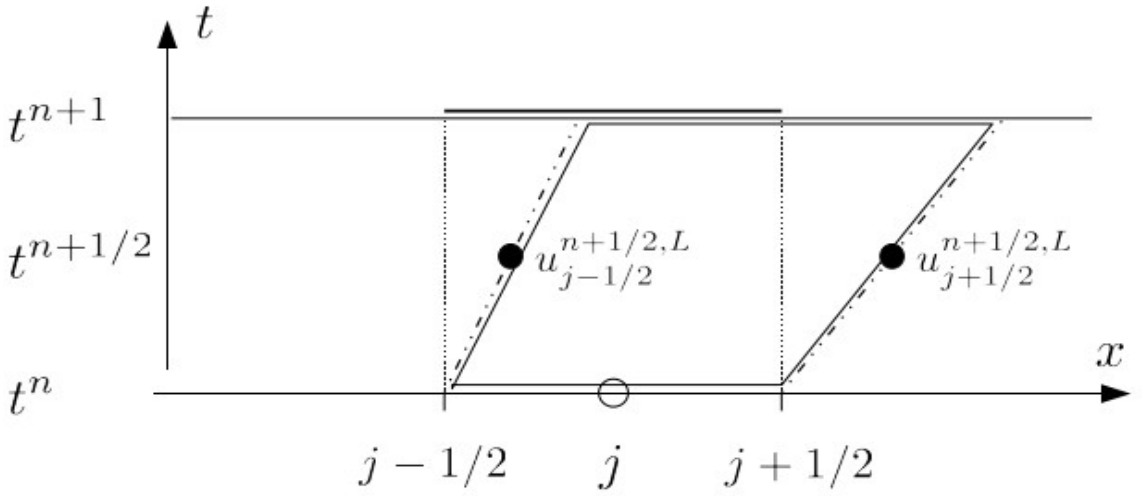

Lagrange-remap: conservative reformulation

Mass balance rewritting : under some convenient CFL condition, we have

$$\begin{aligned} h\rho_j^{n+1} &= h_j^{n+1,L}\rho_j^{n+1,L} - \Delta t \rho_{j+1/2}^{upw,n+1} u_{j+1/2}^{n+1/2,L} + \Delta t \rho_{j+1/2}^{upw,n+1} u_{j-1/2}^{n+1/2,L} \\ &= h\rho_j^n - \Delta t \rho_{j+1/2}^{upw,n+1} u_{j+1/2}^{n+1/2,L} + \Delta t \rho_{j+1/2}^{upw,n+1} u_{j-1/2}^{n+1/2,L} \end{aligned}$$

in the form

$$\rho_j^{n+1} = \rho_j^n - \frac{\Delta t}{h}\left(\Phi_{m,j+1/2}^{n+1/2,n+1} - \Phi_{m,j-1/2}^{n+1/2,n+1}\right),$$

$$\Phi_{m,j+1/2}^{n+1/2,n+1} = \rho_{j+1/2}^{upw,n+1} u_{j+1/2}^{n+1/2,L}.$$

[De Vuyst, Fochesato, Loubère, Saas, Motte, Ghidaglia, preprint paper 2013]

Remark

First-order (1st-order remap) LR schemes are actually 5-point schemes !

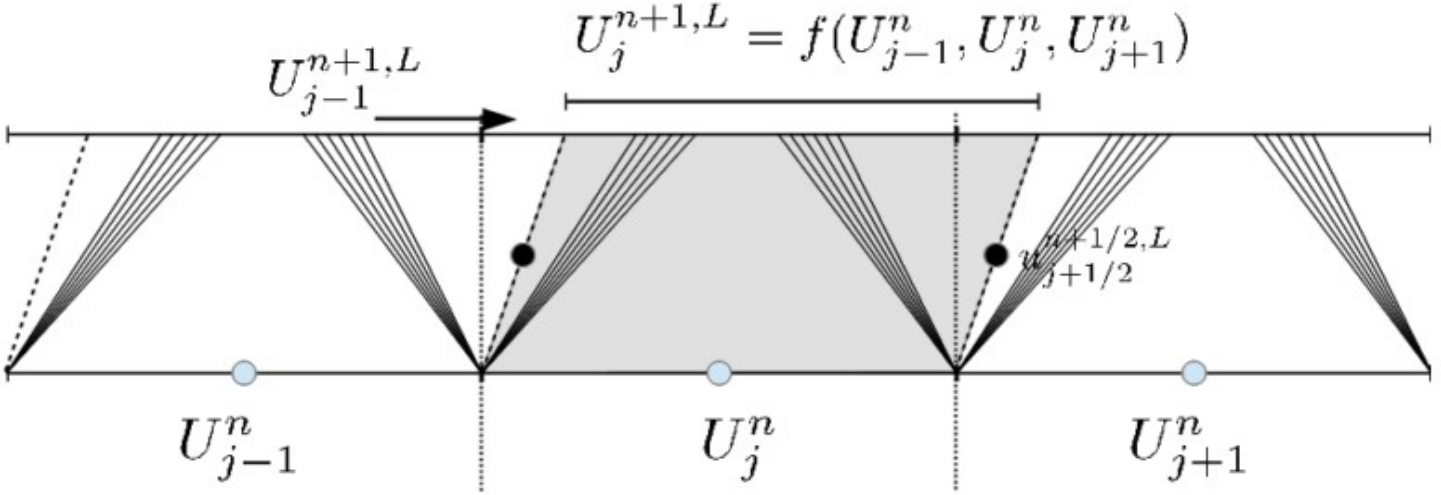

$$U_j^{n+1} = U_j^n - \frac{\Delta t}{h}\left(\Phi_{j+1/2}^{n,n+1} - \Phi_{j-1/2}^{n,n+1}\right),$$

$$\Phi_{j+1/2}^{n,n+1} = \Phi\left(U_{j-1}^n, U_j^n, U_{j+1}^n, U_{j+2}^n, \Delta t\right).$$

→ Large stencil method : limited GPU performance because of lot of memory reads.

Lagrange-remap : two-dimensional case (1st-order accurate)

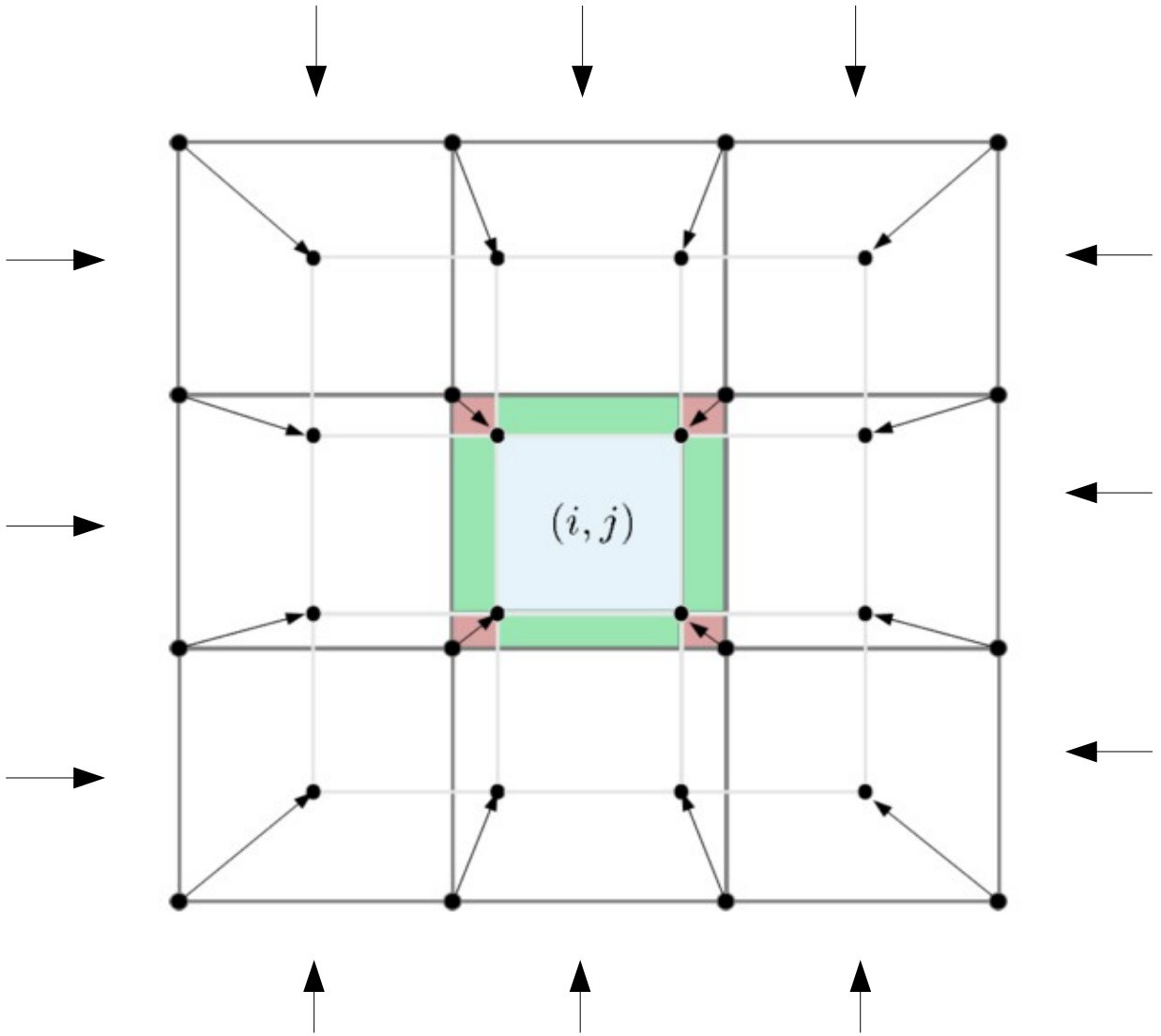

21-point scheme ! (large stencil)
NB : multidimensional corner effects